Available online at www.sciencedirect.com

ScienceDirect

St. Petersburg Polytechnical University Journal: Physics and Mathematics 1 (2015) 109–112

www.elsevier.com/locate/spjpm

Structural features of indium antimonide quantum dots on the indium arsenide substrate

Liliya A. Sokura*, Vladimir N. Nevedomskiy, Nikolay A. Bert

Ioffe Physical Technical Institute of the Russian Academy of Sciences, 26 Politekhnicheskaya St., St. Petersburg, 194021, Russian Federation

Available online 30 July 2015

Abstract

The properties of InSb/InAs quantum dots (QDs) have been investigated by transmission electron microscopy (TEM). Specific features of diffraction contrast were discovered in plan-view TEM images of big (9–10 nm in height and 38–50 nm in diameter) InSb QDs. To understand the origin of such distortions, a model of an InSb QD on InAs substrate containing a partial Frank dislocation (FD) was developed and used for calculations of the displacement field and the subsequent diffraction image simulation of an InSb QD for the first time. The shape of the QD was established to have an insignificant influence on the magnitude of radial displacements. The insertion of a misfit defect (a partial Frank dislocation) into the QD reduces the strain at the edges of the QD almost by 30%. The comparison of experimental and simulated data allowed us to explain the observed features of the moiré pattern in the image of a big InSb QD by the presence of a misfit defect at the QD-substrate interface.

Keywords: Quantum dot; Electron microscopy; Semiconductor; Misfit dislocation.

1. Introduction

Heterostructures based on indium antimonide (InSb) quantum dots (QDs) on gallium antimonide (GaSb) and indium arsenide (InAs) substrates show promise as materials for fabricating optoelectronic mid-IR range devices (3–5 μm). For example, mid-IR range lasers are used in a wide variety of areas, such as chemical process control, environmental monitoring, leakage control, non-invasive medical diagnostics, and laser surgery.

The structural properties of the InSb/InAs system are similar to those of the well-studied InAs/GaAs system. Its crystalline structure also forms a face-centered cubic (fcc) lattice. The lattice mismatch of the InSb/InAs system is 6.9% and is close to that of the InAs/GaAs system (7.2%). However, as the optimal conditions for obtaining InSb quantum dots on InAs substrates have not yet been worked out, large islands containing structural defects are formed in the substrate along with small QDs during QD growth.

The main purpose of this study is to gain insight into the nature of misfit defects in large incoherent InSb/InAs quantum dots. To this end we examined the structure of an InSb/InAs QD using the method of transmission electron microscopy (TEM). Based on the experimental data, we modeled the structure of such QDs to calculate

* Corresponding author.
E-mail addresses: sokura@mail.ioffe.ru (L.A. Sokura), nevedom@mail.ioffe.ru (Vladimir N. Nevedomskiy), Nikolay.Bert@mail.ioffe.ru (Nikolay A. Bert).

http://dx.doi.org/10.1016/j.spjpm.2015.07.002

(Peer review under responsibility of St. Petersburg Polytechnic University).

the displacement field and the diffraction contrast by the finite element method.

2. The experiment

Experimental samples were obtained through liquid phase epitaxy (LPE) and metalorganic vapor phase epitaxy (MOVPE). A QD on an InAs (001) substrate was grown epitaxially in a horizontal LPE system with a standard graphite boat under oxygen flow at temperatures ranging from 420 to 445 °C; the QD growth time was 2 s, and the system cooling rate was 0.3–0.6 °C/min. An InSb/InAs QD was also grown epitaxially in a standard MOVPE reactor under atmospheric pressure, at 420–440 °C and with an atomic indium supply rate of 5.6–8.0 μmol/min. The growth of the QD with these methods is described in detail in [1–5].

To investigate the QD properties by TEM the samples were prepared according to standard procedure of preliminary mechanical thinning followed by ion beam milling (argon ion beam energy was 4 keV). The TEM study was carried out in a JEOL JEM 2100F microscope at an accelerating voltage of 200 kV in the diffraction and high-resolution modes. Both cross-section and plan-view TEM specimen configurations were used.

3. Experimental results

When studying the quantum dots with TEM, we found bimodality in object size distribution. There were small QDs of 5 nm and 18–22 nm in diameter, and also large QDs of 9–10 nm high and 38–50 in diameter. The examination of the QD's cross-section showed that the majority of the QDs were spherical, but there were also some trapeze-shaped QDs.

When we examined the objects in plan-view TEM images under two-beam diffraction conditions, we found a classical moiré pattern for small quantum dots. As discussed in [6,7], such a moiré pattern appears as a result of a significant lattice spacing mismatch and a plastically relaxed non-buried island. Fig. 1 (a) represents an example of this pattern. As within the classical case, the moiré

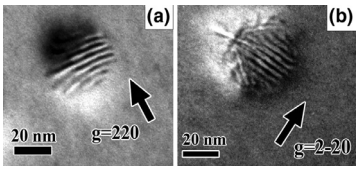

Fig. 1. TEM images of a small (a) and a large (b) InSb/InAs QD in planar geometry with a moiré pattern.

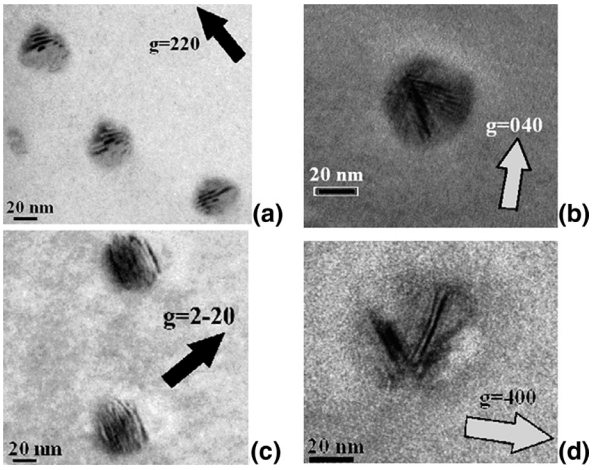

Fig. 2. TEM images of large InSb/InAs QDs under two-beam diffraction conditions.

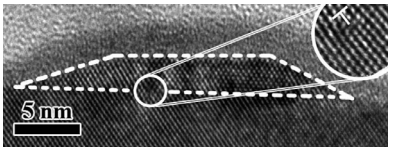

Fig. 3. A high-resolution electron microscopy image of an InSb/InAs QD (marked with a dashed line) with the misfit dislocation (shown on a larger scale).

fringes are perpendicular to the diffraction vector and rotate as the vector turns. It is evident that larger QDs, in contrast to smaller ones, exhibit a complex moiré pattern (Fig. 1 (b)). When the diffraction vector **g** changed direction, the contrast of a large QD did not turn with it, but the pattern itself changed (Fig. 2). The 'ticks' appearing in the image cannot be explained from the simple considerations of moire formation. The observed pattern allows us to conclude that there is no axial symmetry axis (001) in the QD and the planar plane has a preferred direction.

High-resolution electron microscopy images showed a dislocation near the quantum dot/substrate interface. In the images of the cross-section of the QD, this dislocation is visible inside the crystal lattice (Fig. 3). This structural defect can appear as a result of a mismatch between the parameters of the QD lattice and substrate.

4. The diffraction contrast modeling

To find out why a complex moiré pattern appears, we modeled a QD diffraction contrast with a misfit dislocation. To simulate the contrast images from a single InSb on the substrate surface, we constructed a mechanical model of the system and calculated the dislocation fields.

It is known from published data that two types of dislocations are most commonly observed on the <111> planes of an fcc lattice along the QD/substrate interface: a 60-degree dislocation and a partial Frank dislocation (FD). A partial Frank dislocation (FD) often occurring in incoherent QDs in the well-studied InAs/GaAs system [8] was selected to represent a misfit defect in our model. The dislocation lies on the QD/substrate interface along the [110] direction and is characterized by the Burgers vector $\mathbf{b} = 1/3\,[111]$. The dislocation field inside and outside the QD was calculated for the relaxed state of the substrate.

We studied cylindrical, trapeze-shaped and spherical quantum dots. The latter two were observed experimentally.

The results of simulating the dislocation field inside the QD proved that the shape of the QD has little influence on the value and the distribution of the field. Regardless of the QD shape, the presence of an FD in the QD significantly changes the dislocation field distribution in the surrounding area and lowers the dislocation density around the QD edges (by almost 30%).

Fig. 4 shows the results of simulating the dislocation field for a cylindrical QD, which allows to compare the positions of the equal dislocation lines for the two cases: with and without the partial Frank dislocation.

The simulated dislocation fields were used for modeling the diffraction contrast of the TEM images. The images of the FD-containing QDs in planar geometry were calculated from the Howie–Whelan dynamic approximation. This approach is employed for solving problems of electron diffraction in defective crystals, and involves two differential equations for the amplitudes of the transmitted (Φ_0) and the diffracted (Φ_g) electron waves.

$$\frac{d\Phi_o(z)}{dz} = \frac{\pi i}{\xi_g}\Phi_g(z)exp(2\pi i\vec{g}\vec{u})$$

$$\frac{d\Phi_g(z)}{dz} = \frac{\pi i}{\xi_g}\Phi_o(z)exp(-2\pi i\vec{g}\vec{u}) + 2\pi i\vec{s}\Phi_g(z),$$

where $\vec{g}$ is the diffraction vector, ξ_g is the extinction length, s is the deviation parameter ($s = 0$ for our calculations) [9,10].

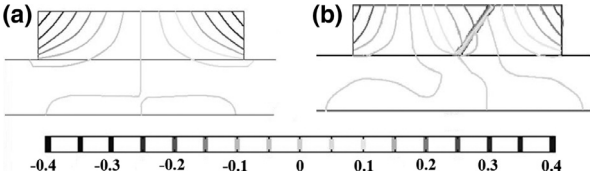

Fig. 4. shows the results of simulating the dislocation field for a cylindrical QD, which allows to compare the positions of the equal dislocation lines for the two cases: with and without the partial Frank dislocation.

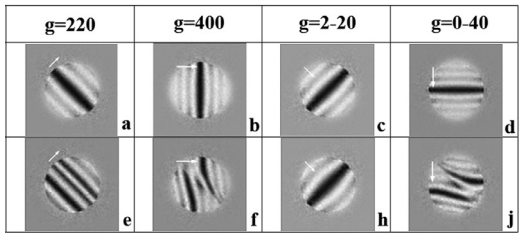

Fig. 5. The results of modeling the diffraction contrast from the quantum dots without (a–d) and with (e–j) the partial Frank dislocation; the lattice mismatch between the substrate and the QD is 3%. White arrows show the direction of the diffraction vector.

5. Discussion of the results

The results of the contrast calculations showed that the island shape has obviously no influence on the resulting diffraction contrast. The image of the diffraction contrast, however, depends on the value of the mismatch between the QD and substrate lattice parameters (Fig. 5). The moiré pattern also changes considerably with diffraction vector rotation.

The addition of an FD into a QD leads to various changes in the moiré pattern. As can be seen in Fig. 5, additional moiré bands fringes appear on the contrast with the operating diffraction vector $g = 220$. The dislocation inside the QD also, apparently, has no effect on the diffraction contrast with the vector $g = 2–20$.

An increase in the lattice mismatch between the parameters of the QD and substrate lattices leads to a decrease in the moire period and, consequently, to an increase in the number of fringes.

The comparison of the modeled and the experimental images (Fig. 6) showed that the experimental images for small QDs for $g = 220$ (see Fig. 6 (d)) match the simulations in moiré period and the number of moiré

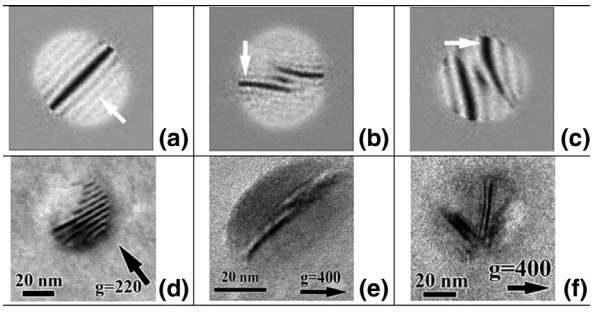

Fig. 6. The comparison of the modeled (a–c) and experimental (d–f) contrast images in an InSb QD without (a) and with (b–c) the partial Frank dislocation; the lattice mismatch between the QD and the substrate is 3% (c, f) and 6% (a, b, d, e); the diffraction vector g is: 220 and 2–20 (a, d), 400 and 0–40 (b, c, e, f).

fringes with a 6% lattice mismatch (Fig. 6 (a)). This means that small QDs consist of pure indium antimonide and have no arsenic inclusions (or a small amount of it).

For a 3 and a 6% mismatch distinctive 'ticks' (Fig. 6 (b) and (c)) can be observed in simulated contrast images with the diffraction vector $g = 400$ and 0–40; the same 'ticks' appear in experimental TEM images of large QDs (Fig. 6 (e) and (f)). This proves that misfit defects are present on the quantum dot/substrate interface for larger QDs.

6. Conclusions

We have studied the structure of an unburied indium antimonide quantum dot on an indium arsenide substrate by transmission electron microscopy and computer modeling of the EM images. Moiré pattern features were discovered for the diffraction contrast of larger QDs (9–10 nm in height and 38–50 nm in diameter). To understand the reasons of the complex moiré pattern appearing in TEM images, a model of an indium antimonide QD on an indium arsenide substrate was constructed for the first time and subsequently used to calculate the dislocation fields and simulate the diffraction contrast.

We found that the shape of a QD has an insignificant influence on the size of radial dislocations in the system. The inclusion of a misfit defect (partial Frank dislocation) into a QD during structure modeling lessens the strains on the QD borders almost by 30%.

The simulated images of the QD with Frank dislocations on the QD/substrate interface are in good agreement with the experimental EM images. This serves as definitive prove that the Frank dislocation is present in the quantum dot, which helps explain the experimentally observed features of the moiré pattern from the quantum dot.

Acknowledgments

The authors are grateful to K.D. Moiseev for providing us with samples and for many fruitful discussions.

References

[1] V.V. Romanov, P.A. Dementyev, K.D. Moiseyev, Specific features of nanosize object formation in an InSb/InAs system by metal-organic vapor-phase epitaxy, Semiconductors 47 (2013) 443–448.

[2] K.D. Moiseyev, Ya.A. Parkhomenko, Ye.V. Gushchina, A.V. Ankudinov, M.P. Mikhaylova, N.A. Bert, Yu.P. Yakovlev, Specific features of the epitaxial growth of narrow-gap InSb quantum dots on an InAs substrate, Semiconductors 43 (2009) 1102–1109.

[3] K.D. Moiseyev, Ya.A. Parkhomenko, A.V. Ankudinov, Ye.V. Gushchina, M.P. Mikhaylova, A.N. Titkov, Yu.P. Yakovlev, InSb/InAs quantum dots grown by liquid phase epitaxy, Tech. Phys. Lett. 33 (2007) 295–298.

[4] M. Mikhailova, N. Stoyanov, I. Andreev, B. Zhurtanov, S. Kizhaev, E. Kunitsyna, K. Salikhov, Yu. Yakovlev, Optoelectronic sensors on GaSb- and InAs- based heterostructures for ecological monitoring and medical diagnostics, in: Proceedings of SPIE on Optical Sensing Technology and Applications, 6585, 2007 658526–9.

[5] N.A. Bert, V.N. Nevedomsky, P.A. Dement'ev, K.D. Moiseev, TEM-study of free-standing self-assembled InSb quantum dots grown on InAs surface, Appl. Surf. Sci. 267 (2013) 77–80.

[6] N.A. Bert, A.B. Freidin, A.L. Kolesnikova, I.K. Korolev, A.E. Romanov, On strain state and pseudo-moire TEM contrast of InSb quantum dots coherently grown on InAs surface, Phys. Status Solidi A-Appl. Mat. 207 (2010) 2323–2326.

[7] Y. Androussi, T. Benabbas, A. Lefebvre, Moiré-like fringes in transmission electron microscopy images of coherently strained semiconductor islands, Ultramicroscopy 93 (2002) 161–167.

[8] Y. Chen, X.W. Lin, Z. Liliental-Weber, J. Washburn, J.F. Klem, J.Y. Tsao, Dislocation formation mechanism in strained InxGa1−xAs islands grown on GaAs(001) substrates, Appl. Phys. Lett. 68 (1996) 111–113.

[9] P. Hirsch, A. Howie, R.B. Nicholson, D.W. Pashley, M.J. Whelan, Electron Microscopy of Thin Crystals, Robert E. Krieger Publishing, New York, 1968.

[10] David B. Williams, C. Barry Carter, Transmission Electron Microscopy, A Textbook for Materials Science, Part 2, Plenum Press, New York, 2009.